UDK 52-726:662.2.032:691.714
Original scientific article/Izvirni znanstveni članek

ISSN 1580-2949
Mater. Tehnol.

INFLUENCE OF PLASMA NITRIDING PARAMETERS ON THE MECHANICAL PROPERTIES OF 25Cr2Ni4W STEEL

VPLIV PARAMETROV PLAZMENSKEGA NITRIRANJA NA MEHANSKE LASTNOSTI JEKLA 25 CR2Ni4W

Brahim Chermime[1*], Ouafa Hamidane[2], Mohammed Mounes Alim[3], Mamoun Fellah[4]

[1,2,4]Mechanical Department, University Abbes Laghrour Khenchela, Khenchela 40000, Algeria
[3]Centre de Développement des Technologies Avancées, Cité 20 Aout 1956, B.P. 17, Baba Hassan, Alger 16000, Algeria
[1*,2]Laboratory of Engineering and Sciences of Advanced Materials (ISMA), Khenchela 40000, Algeria

Prejem rokopisa – received: 2025-02-24; sprejem za objavo – accepted for publication: 2025-08-26

doi:10.17222/mit.2025.1411

In this study, plasma nitriding was applied to 25Cr2Ni4W low-alloy steel to improve its mechanical and tribological surface properties. The investigation focused on varying the negative bias voltage while keeping the discharge power, pressure, and holding time constant. The substrate temperature increased due to the self-induced heating mechanism. The compound layer of the treated samples revealed the formation of nitride phases (ε-$Fe_{2-3}N$ and γ'-Fe_4N), as observed through XRD analysis and optical microscopy. A phase transition was noted between 2.0 kV and 3.5 kV, accompanied by an increase in the volume fraction of the γ'-Fe_4N phase and a decrease in the volume fraction of the ε-$Fe_{2-3}N$ phase. When comparing the nitrogen-implanted samples to their untreated counterparts, an increase in nanohardness was observed, suggesting that the nitride phases contributed to the hardening.

Keywords: plasma nitriding, low alloy steel, tribology, nanohardness

V članku avtorji opisujejo študijo uporabe plazemskega nitriranja malo legiranega jekla vrste 25Cr2Ni4W, da bi izboljšali mehanske in tribološke lastnosti njegove površine. Preiskava se je osredotočila na spreminjanje nivoja napetosti pri konstantni moči, tlaku in času zadrževanja. Zaradi učinka obdelave s plazmo se je površina substrata (obdelovanca) segrevala. Rentgenska strukturna analiza (XRD) in pregled pod svetlobnim mikroskopom (OM) sta pokazala, da je nastala prevleka, ki je bila sestavljena iz nitridnih faz ε-$Fe_{2-3}N$ in γ'-Fe_4N. Avtorji so opazili fazni prehod med 2,0 kV in 3,5 kV, ki je bil posledica večanja prostorskega deleža faze γ'-Fe_4N in manjšanja prostorskega deleža faze ε-$Fe_{2-3}N$. Primerjava nitriranih vzorcev z nenitriranimi je pokazala znatno povečanje nanotrdote njihove površine zaradi izvedenega plazemeskega nitriranja in nastanka nitridne plasti debeline od 28 µm do 31 µm.

Ključne besede: plazemsko nitriranje, malolegirano jeklo, tribologija, nanotrdota

1 INTRODUCTION

Alloying elements in low-alloy steel, such as chromium, molybdenum, and nickel, can be added, provided that the total percentage of these additions is less than 10 %.[1] After heat treatment, these alloying elements enhance the mechanical properties of the steel, particularly in terms of hardness and toughness.[2] To increase creep strength, low-alloy steels typically contain 0.5–1 % molybdenum. Additionally, chromium (0.5–9 %) is added to improve resistance to graphitization, corrosion, and rupture.[3]

Given the widespread use of steel in various industries and the continuous advancement of mechanical production, the development of surface characteristics has become increasingly important. This requires the use of surface treatments, such as plasma nitriding. This is a thermochemical surface treatment commonly applied to tools and mechanical parts. When performed at temperatures lower than the AC1 temperature on the phase diagram, the process does not cause phase changes in the base material, thus preserving its inherent properties. During this process, the creation of nitrides and interstitially located atoms leads to lattice deformation, which increases the material's hardness.[4]

Plasma nitriding enhances tribological properties, fatigue strength, wear resistance, and surface corrosion resistance of steel while maintaining its core properties.[5–10] The process uses "cold" plasma, which is plasma out of thermodynamic equilibrium. In this type of plasma, the temperature of ions and neutrals is close to room temperature and much lower than that of electrons (10^4–10^5 K). Cold plasmas can serve as a source of photons (e.g., lamps, plasma screens or active species for applications such as surface treatments pollution control,[11–15] chemical synthesis, materials analysis and sterilization.[16–18]

Despite its numerous advantages, such as reduced environmental impact, high diffusion speed, and low energy consumption, plasma nitriding faces certain challenges, including difficulty in achieving reproducible

*Corresponding author's e-mail:
Chermime.Brahim@univ-khenchela.dz (Brahim Chermime)

properties in nitrided parts, surface distortions due to arcing, and overheating of small components.[19]

2 EXPERIMENTAL PART

2.1 Materials description

The low-alloy steel 25Cr2Ni4W, used in this study, is widely used in the manufacturing of pipes, railway rails, automobile and aircraft bodies, as well as in onshore and offshore structural engineering. The chemical composition of this low-alloy steel is detailed in **Table 1**. The presence of nickel and chromium provides the 25Cr2Ni4W steel with excellent tensile strength, wear resistance, and high ductility, while manganese enhances its hardenability.

Nanoindentation tests were carried out using a CSM Instruments nanoindenter equipped with a Berkovich diamond indenter. A maximum load of 200 mN was applied in a continuous loading–unloading cycle, resulting in a penetration depth of approximately 2000 nm. The surface roughness of the samples prior to testing was about $R_a \approx 0.05$ μm, which is sufficiently low to minimize roughness effects on the indentation response. For each experimental condition, at least ten indents were performed to ensure statistical reliability. Load–displacement curves were analysed in accordance with the Oliver–Pharr method, focusing on the unloading portion of the curve to determine hardness (H) and reduced elastic modulus (E_{eff}).

Table1: Chemical composition of 25Cr2Ni4W

Component	C	Si	Mn	Cr	Ni	W	P	S
w/%	0.28	0.16	0.5	1.52	3.97	0.73	0.025	0.012

2.2 Plasma nitriding processing

Figure 1 demonstrates the experimental configuration utilized for the plasma nitriding. It is made up of a 930 mm-diameter spherical chamber that is attached to a pumping device to remove air up to a vacuum of 10^{-3} mTorr. The main pump in this system may achieve a vacuum of approximately 1 mTorr, while a secondary oil diffusion pump is used to further decrease the pressure and maintain high-vacuum conditions.

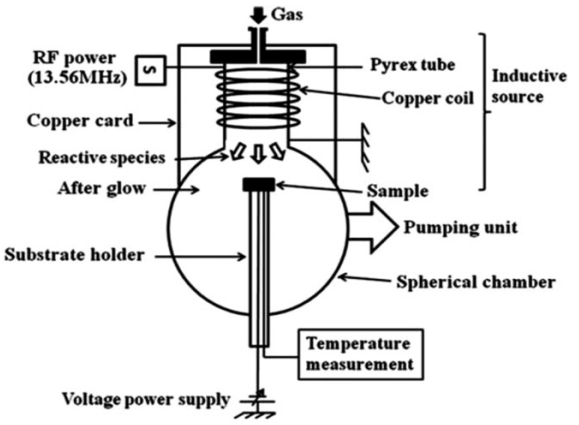

Figure 1: Inductive source installed on one of the vacuum chamber accesses[20]

An in-house-produced inductively coupled plasma (ICP) source was encircled by a copper coil that was polarized at 13.56 MHz using an RF generator. The Pyrex tube had dimensions of (170, 100 and 5) mm. A braid-insulated quartz substrate holder, measuring 1500 mm in length and 13 mm in diameter, was employed to avert electrical breakdown and arcing issues resulting from the DC bias voltage. High negative voltage power supply (HCN 2800–6500) was utilized to bias our samples to 400 mA/6.5 kV or higher values.[20–22] A sample and the plasma source were spaced 100 mm apart for each treatment in order to achieve surface homogeneity. Initially, the chamber was evacuated to a base pressure of about 10^{-3} mTorr. Nitrogen was then added to the system to bring the operating pressure to 20 mTorr. The native oxide layer on the substrate top surface was sputter-deposited using argon gas for 30 min at a discharge power of 200 W, prior to the initiation of ion implantation. With a voltage range of 2–3.5 kV and a current of roughly 7–20 mA, the substrate was negatively biased. An AK-type thermocouple was used to measure the substrate temperature.

Table 2: Parameters of the experiment

Parameter	Value
First pressure	3.10^{-5} mbar
Power	400 Watt
Negative bias voltage	3.5 KV
Holding time	60 min

2.3 Microstructure of a sample

Figure 2 shows our steel in the untreated state, having a globular pearlite structure and some primary carbides of more or less rounded morphology.

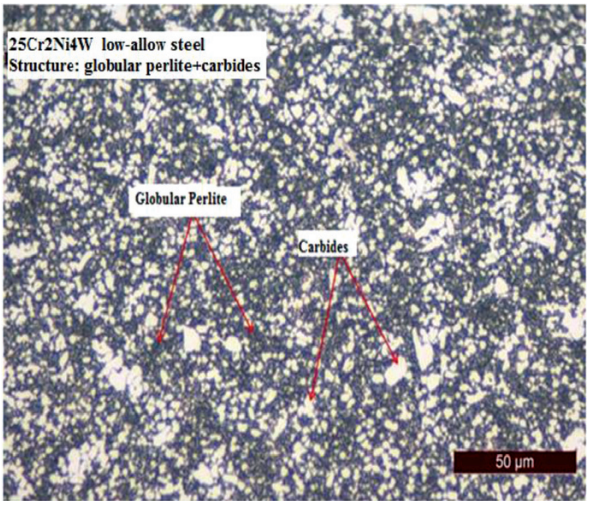

Figure 2: Micrograph of untreated 25Cr2Ni4W steel

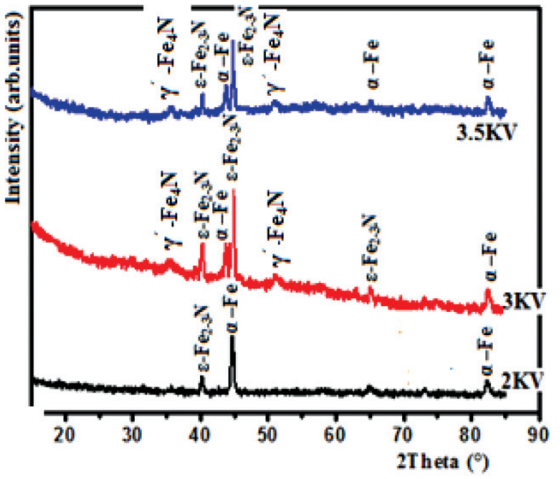

Figure 3: XRD patterns of plasma-nitrided samples

3 RESULTS AND DUSCUSSION

3.1 X-ray diffraction analysis

Figure 3 presents the XRD diagram of the sample subjected to a 2 kV polarization, revealing three peaks at 40.3°, 44.9°, and 81.75°, corresponding to the ε-$Fe_{2-3}N$, α-Fe, and parent α-Fe phases. At 3.0 kV and 3.5 kV, these phases are still observed, but the peak at 44.9° significantly decreases.

The sample treated at 3.0 kV shows weak peaks at 35.7° and 51.8°, attributed to the γ'-Fe_4N phase, as well as a peak at 65.6° linked to the ε-$Fe_{2-3}N$ phase, likely due to a reduction in the nitrogen content, modifying its lattice parameter. At 3.5 kV, a peak at 58.7° is identified as α-Fe_2O_3, suggesting increased self-heating, which enhances nitrogen diffusion but reduces its concentration in the treated layer. The presence of γ'-Fe_4N at 3.5 kV is associated with diffusion phenomena, confirming the presence of ε-$Fe_{2-3}N$ and γ'-Fe_4N phases in accordance with the Fe-N binary phase diagram.[23] Finally, the formation of a thin Fe_2O_3 oxide layer at 3.5 kV is attributed to the high temperatures reached under these conditions.

3.2 Nanoindentation measurements

Figure 4 shows the variation in nanohardness over time, highlighting the significant influence of the applied voltage during nitriding treatment on the sample.

At 2 kV, the nanohardness gradually increases, indicating a progressive structural improvement. Under 3 kV, this increase is more pronounced, suggesting a faster densification of the material due to enhanced atomic mobility. At 3.5 kV, the trend continues with an even more significant rise in hardness, indicating a more effective strengthening of the material under higher voltage. These results show that the intensity of the electric field during nitriding plays a key role in the evolution of hardness, directly affecting the material's compactness and mechanical resistance over time.

3.3 Young's modulus of the treated and untreated samples

Figure 5 shows the effect of plasma nitriding at 2 kV, 3 kV, and 3.5 kV on the Young's modulus of low-alloy steel for 90 minutes, compared to an untreated sample. While the untreated sample remains stable, the nitrided samples exhibit initial fluctuations (20–30 min) due to nitride layer formation and measurement sensitivity. After this phase, their Young's modulus stabilizes, aligning with the untreated material. This indicates that plasma nitriding primarily affects surface properties, especially hardness, with a minimal impact on the bulk modulus. The slight variations confirm that the treatment's influence is superficial, preserving the material's overall stiffness.

3.4 Nitrided layer thickness

Figure 6 shows that the measured nitrided layer thickness ranges between 28.138 μm and 31.026 μm,

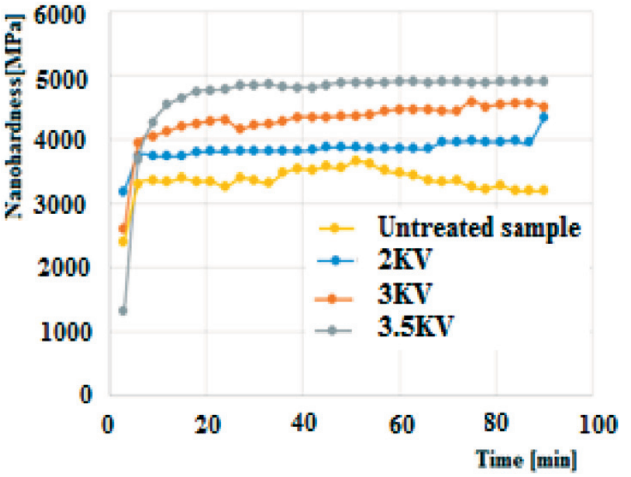

Figure 4: Nanohardness (MPa) measurement of the treated and untreated steel

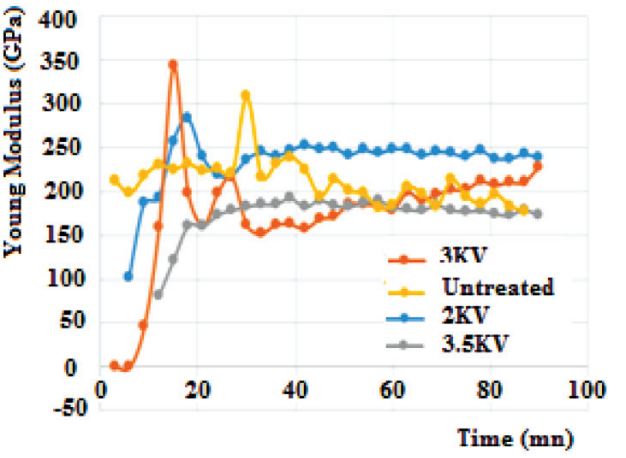

Figure 5: Young's modulus of the treated and untreated samples

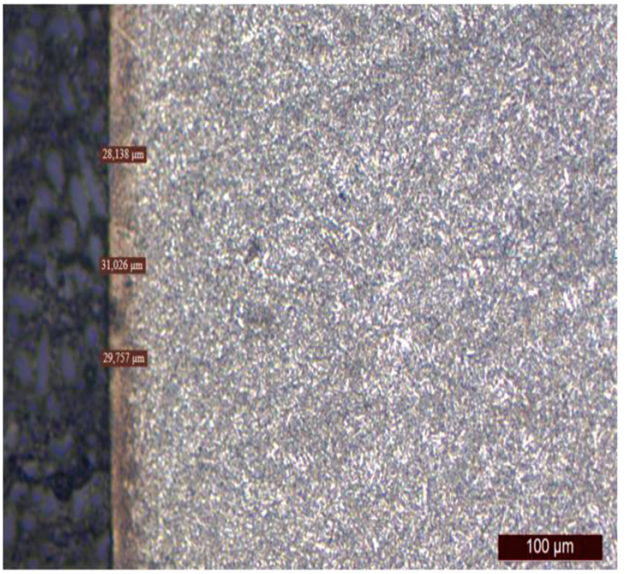

Figure 6: Nitriding layer varying from 28.138 µm to 31.026 µm

aligning well with literature values. For instance, Smith et al. (2018) reported thicknesses from 25 µm to 40 µm for gas-nitrided low-alloy steel. Miller and Zhang (2020) found ranges between 30 µm and 50 µm for plasma nitriding, while Gomez et al. (2016) observed values between 20 µm and 35 µm, depending on treatment conditions. These slight variations across studies are attributed to the differences in nitriding temperature, duration, and steel composition, confirming that our nitriding process is both effective and well-optimized.

4 CONCLUSIONS

This study confirms that plasma nitriding is an effective surface treatment for enhancing the mechanical and tribological properties of 25Cr2Ni4W low-alloy steel. By carefully adjusting the negative bias voltage, the process produces a well-optimized nitrided layer characterized by the formation of ε-$Fe_{2-3}N$ and an increased presence of γž-Fe_4N phase, as demonstrated with the XRD analysis. This controlled nitride layer plays a pivotal role in achieving rapid surface hardening, particularly within the first 20 minutes of treatment, and in redistributing stress across the material, thereby improving wear resistance and potentially enhancing fatigue life. Moreover, the treatment primarily enhances the steel's surface properties without significantly affecting its bulk mechanical integrity. These promising results lay the groundwork for further optimization of plasma nitriding parameters and encourage future investigations into the long-term performance of treated low-alloy steels in real-world applications.

Acknowledgment

We would like to express our sincere gratitude to the CDTA laboratory in Algiers for conducting the tests, as well as to Khechela Mechanical Construction Company for their invaluable support in preparing the samples and carrying out several additional tests.

5 REFERENCES

[1] W. D. Callister, Materials Science and Engineering: An Introduction, John Wiley, 2007

[2] ASM Handbook Committee, Properties and Selection: Irons, Steels, and High-Performance Alloys, ASM International, 1990

[3] F. Masuyama, Low-alloyed steel grades for boilers in ultra-supercritical power plants, in: A. Di Gianfrancesco (Ed.), Materials for Ultra-Supercritical and Advanced Ultra-Supercritical Power Plants, Woodhead Publishing, 2017, 53–76

[4] K.-M. Winter, J. Kalucki, D. Koshel, Process technologies for thermochemical surface engineering, in: Thermochemical Surface Engineering of Steels, 2015, 141–206

[5] A. R. West, Solid State Chemistry and its Applications, John Wiley & Sons, 2014

[6] H. A. Wriedt, N. A. Gokcen, R. H. Nafziger, The Fe–N (Iron–Nitrogen) system, Bull. Alloy Phase Diagr., 8 (**1987**), 355

[7] M. Sommer, et al., Variation of the compound layer structure by controlled gas nitriding and nitrocarburizing, HTM J. Heat Treatm. Mat., 77 (**2022**), 214–227, doi:10.1515/htm-2022-1011

[8] S. Thibault, et al., A simple model for hardness and residual stress profiles prediction for low-alloy nitrided steel, based on nitriding-induced tempering effects, HTM – J. Heat Treatm. Mat., 73 (**2018**), 235–245, doi:10.3139/105.110360

[9] A. Gramlich, et al., Plasma Nitriding of an Air-Hardening Medium Manganese Forging Steel, HTM – J. Heat Treatm. Mat., 77 (**2022**), 298–315, doi:10.1515/htm-2022-1017

[10] M. S. Aggoune, L. Torchane, Optimization and control of gaseous nitriding of a 33CrMoV12-9 steel, J. Mater. Testing., (2023)

[11] P. A. Kruglenya, O. Y. Maslennikov, Advanced structure of cathode for gas discharge lamp of super high pressure, Appl. Surf. Sci., 215 (**2003**), 101–104

[12] H. Oyama, N. Shiramatsu, Smaller and bigger displays, Displays, 23 (**2002**), 31–39

[13] D. Sun, G. K. Stylios, Fabric surface properties by low temperature plasma treatment, J. Mat. Proc. Technol., 173 (2006), 172–177

[14] S. Y. Park, B. R. Deshwal, S. H. Moon, NOx removal from the flue gas of oil-fired boiler using a multistage plasma-catalyst hybrid system, Fuel Proc. Technol., 89 (**2008**), 540–548

[15] F. Rousseau, S. Awamat, M. Nikravech, D. Morvan, J. Amouroux, Deposit of dense YSZ electrolyte and porous NiO–YSZ anode for SOFC device by a low pressure plasma process, Surf. Coat. Technol., 202 (**2007**), 1226–1230

[16] A. Brysbaert, K. Melessanaki, D. Anglos, Pigment analysis in Bronze Age Aegean and Eastern Mediterranean painted plaster by laser-induced breakdown spectroscopy (LIBS), J. Archaeol. Sci., 33 (**2006**), 1095–1104

[17] M. Moisan, J. Barbeau, S. Moreau, J. Pelletier, M. Tabrizian, L'H. Yahia, Low-temperature sterilization using gas plasmas: a review of the experiments and an analysis of the inactivation mechanisms, Int. J. Pharmaceutics, 226 (**2001**), 1–21

[18] Z. Xu, F. F. Xiong, Plasma Surface Metallurgy, Springer, 2008

[19] Y. Sun, E. Haruman, Effect of carbon addition on low-temperature plasma nitriding characteristics of austenitic stainless steel, Vacuum, 81 (**2006**), 114–119

[20] Y. Setrsuhara, S. Miyake, Y. Sakawa, T. Shoji, Surf. Coat. Technol., 136 (**2001**) 60

[21] A. Anders, Plasma and ion sources in large area coating: A review, Surf. Coat. Technol., 200 (**2005**), 1893

[22] Z. J. Wang, X. B. Tian, C. Z. Gong, J. W. Shi, S. Q. Yang, R. K. Y. Fu, P. K. Chu, Plasma immersion ion implantation into cylindrical

bore using internal inductively coupled radio-frequency discharge, Surf. Coat. Technol., 206 (**2012**), 5042